C Journal of Carbon Research

MDPI

Article

Electrochemical Properties of Graphene Oxide Nanoribbons/Polypyrrole Nanocomposites

Johara Al Dream [1], Camila Zequine [1], K. Siam [1], Pawan K. Kahol [2], S. R. Mishra [3] and Ram K. Gupta [1,4,*]

1 Department of Chemistry, Pittsburg State University, Pittsburg, KS 66762, USA; KAS8000262@gmail.com (J.A.D.); camilazequine@hotmail.com (C.Z.); ksiam@pittstate.edu (K.S.)
2 Department of Physics, Pittsburg State University, Pittsburg, KS 66762, USA; pkahol@pittstate.edu
3 Department of Physics and Materials Science, The University of Memphis, Memphis, TN 38152, USA; srmishra@memphis.edu
4 Kansas Polymer Research Center, Pittsburg State University, Pittsburg, KS 66762, USA
* Correspondence: rgupta@pittstate.edu; Tel.: +1-620-2354-763; Fax: +1-620-2354-003

Received: 5 February 2019; Accepted: 8 April 2019; Published: 12 April 2019

Abstract: Graphene is a highly studied material due to its unique electrical, optical, and mechanical properties. Graphene is widely applied in the field of energy such as in batteries, supercapacitors, and solar cells. The properties of graphene can be further improved by making nanocomposites with conducting polymers. In this work, graphene oxide nanoribbons (GONRs) were synthesized by unzipping multiwall carbon nanotubes. Graphene nanoribbons were used to make nanocomposites with polypyrrole for energy storage applications. The synthesized nanocomposites were structurally and electrochemically characterized to understand their structure and electrochemical properties. The electrochemical characterizations of these nanocomposites were carried out using cyclic voltammetry. The specific capacitance of the nanocomposites was observed to decrease with increasing scan rates. The highest specific capacitance of 2066 F/g was observed using cyclic voltammetry for the optimized nanocomposite of GONR and polypyrrole. Our study suggests that the electrochemical properties of graphene or polypyrrole can be improved by making their composites and that they could be successfully used as electrode materials for energy storage applications. This study can also be extended to the self-assembly of other conducting polymers and graphene nanoribbons through a simple route for various other applications.

Keywords: carbon nanotubes; graphene oxide nanoribbons; polypyrrole; nanocomposites; supercapacitors

1. Introduction

In recent decades, the fast growth of the global economy, a constant diminution of fossil fuels, and increased pollution in the environment have led to an ever-increasing demand for clean energy [1,2]. For the storage and conversion of electrochemical energy, supercapacitors are a preferable choice because of their high power capacity, low cost, environmental friendliness, and long cycle life [3,4]. One of the extremely suitable materials for supercapacitors is graphene [5]. It possesses useful characteristics such as being light in weight while having high electrical conductivity, exceptional mechanical strength, and a large surface area [6]. Nanotubes are also made using graphene sheets that are rolled up, while the football-shaped molecules of fullerenes are spherically wrapped-up graphene. All these different forms of graphene have been utilized in many different applications. However, their electrical and magnetic properties, as well as their elastic behavior have recently captured the attention of researchers.

Graphene oxide nanoribbons (GONRs) are one-dimensional structures of graphene that are typically obtained by unzipping carbon nanotubes (CNTs). Their magnetic and electronic properties

have been studied and explored. Their electronic properties have a diverse range, including normal semiconductors to spin-polarized half metals, and they have the potential of opening GONRs as electric devices [7–9]. Other materials, such as conducting polymers (CPs), are also promising candidates for supercapacitors because of their low cost, higher capacity to store charges, and facile synthesis. Unfortunately, conducting polymers suffer from instability and their life cycle is therefore limited. The working potential range of the CP electrode is limited by degradation due to oxidation during long-term charge–discharge processes and, as a consequence, their conducting properties are gradually reduced [10,11]. The most significant p-type CP is polypyrrole. Polypyrrole has been used for energy storage applications because of its fast redox reaction, high conductivity, high energy density, and low cost [12,13]. It is also used in gas sensors, wires, and polymeric batteries [14–16]. Polypyrrole is also used in making composites with carbon-based materials [17]. In this condition, combining conducting polymers with the carbon material could be a suitable plan and method to gain an ideal capacitive characteristic and for application in energy storage devices.

Tran et al. used polyaniline and polypyrrole in combination with reduced graphene oxide to form a hybrid aerogel for supercapacitor application [18]. The synthesized hybrid aerogel, poly(aniline-co-pyrrole)/graphene aerogel showed a specific capacitance of 675 F/g at 0.5 A/g with outstanding cycling stability and Coulombic efficiency. Sun et al. have synthesized a self-standing nanocomposite foam of polyaniline/reduced graphene oxide for flexible supercapacitors [19]. The polyaniline/reduced graphene oxide-based supercapacitor showed a specific capacitance of 701 F/g at 1 A/g, with high cycling stability. The nanocomposite retained about 92% of its initial specific capacitance after 1000 cycles of charge–discharge study. A novel liquid/liquid interfacial polymerization method was developed to synthesize polypyrrole/graphene oxide nanocomposites [20]. The composites showed improved electrical conductivity and electrochemical reversibility with application in electrochemical energy storage devices. Li et al. fabricated and characterized free-standing polypyrrole/graphene oxide nanocomposite paper for supercapacitor applications [21]. The nanocomposite showed a specific capacitance of about 330 F/g at a scan rate of 100 mV/s with 91% retention in its charge storage capacity after 700 cycles. Konwer et al. used an in-situ polymerization method to synthesize polypyrrole/graphene oxide composite [22]. The synthesized composite showed significant improvement in DC electrical conductivity and charge storage capacity. An in-situ photopolymerization method was used for the synthesis of polypyrrole/reduced graphene oxide composites for energy storage applications [23]. Electrochemical studies showed a specific capacitance of 376 F/g at a scan rate of 25 mV/s for the composite. Zhu et al. used a one-step co-electrodeposition method to prepare polypyrrole/graphene oxide nanocomposite and observed the nanocomposite synergistic effect of polypyrrole and graphene oxide in energy storage capabilities [24]. Multilayered nanoarchitectures of graphene nanosheets and polypyrrole nanowires were developed for high-performance supercapacitors [17]. The multilayer nanoarchitecture of graphene nanosheets and polypyrrole nanowires displayed a specific capacitance of ~165 F/g with high electrochemical cyclic stability.

In this study, we synthesized graphene nanoribbons by unzipping carbon nanotubes and graphene nanoribbons/polypyrrole composites to study the effect of composition on the structural and electrochemical properties for energy applications. It was observed that the electrochemical properties of the nanocomposite were significantly higher than their counterparts.

2. Experimental Details

Multiwall CNTs (MWCNTs) with an outer diameter of 110–170 nm and with length of 5–9 μm were purchased from Sigma-Aldrich, (St. Louis, MO, USA). Sulfuric acid, phosphoric acid, hydrochloric acid, potassium permanganate, and hydrogen peroxide was purchased from Fisher Scientific, Hampton, NH, USA. Ethanol, diethyl ether, polypyrrole, and ferric chloride were also purchased from Fisher Scientific, Hampton, NH, USA. Graphene nanoribbons were synthesized by unzipping CNTs. For this, 1 g of MWCNTs was dispersed in concentrated sulfuric acid (280 mL) and concentrated phosphoric

acid (32 mL). In this, 10 g of potassium permanganate was slowly added under vigorous stirring. The reaction was carried out at 65 °C for 4 h. After that, the reaction mixture was cooled to room temperature and poured over ice water (800 mL) containing hydrogen peroxide (40 mL, 30%). The resulting mixture was congealed for 10 h, filtered through 0.2 μm filter paper (PTFE from Millipore, Burlington, MA, USA) and washed in succession with hydrochloric acid (30%), ethanol (100%), and diethyl ether (anhydrous). The final black material was dried at low heat (65 °C) in a vacuum oven for 10 h.

Polypyrrole was synthesized using a chemical polymerization process. First, pyrrole (0.8 mol) was dissolved in 30 mL of a water/ethanol mixture (1:1, *v*/*v*) and then sonicated for 30 min, followed by the addition of ferric chloride solution (0.8 mol ferric chloride in 20 mL of water) dropwise under vigorous stirring for 24 h. Finally, the obtained material was washed several times with a mixture of water and ethanol until the solution became colorless, and this was dried in a vacuum at 75 °C for 24 h.

For the synthesis of nanocomposites, first, synthesized graphene nanoribbons were dispersed in 50 Ml deionized (DI) water under ultrasonication for 30 min. In another beaker, pyrrole (0.08 mol) was dissolved in 30 mL of a 1:1 water:ethanol mixture. The resultant solution was then added to the dispersion of graphene nanoribbons under ultrasonication for another 30 min. After that, ferric chloride solution (0.04 mol ferric chloride in 20 mL of water) was added dropwise to the above mixture under vigorous stirring for 24 h. The polypyrrole (PPy)/GONR composites obtained were washed several times with a mixture of water and ethanol until the solution became colorless, and were dried in a vacuum at 75 °C for 24 h. The weight ratios of pyrrole to graphene nanoribbons were varied as 99.5:0.5, 98.5:1.5, and 97:3. The resulting nanocomposites were denoted as 0.5 PPyGONR, 1.5 PPyGONR, and 3 PPyGONR. For comparison, the neat PPy was also polymerized by a similar method without the addition of GONRs.

The synthesized materials were characterized using a variety of techniques such as scanning electron microscopy (SEM), X-ray diffraction (XRD), thermogravimetric analysis (TGA), Raman spectroscopy, and electrochemical measurements. The surface morphologies of the MWCNTs, GONRs, PPy, and PPyGONR nanocomposites were characterized using SEM (QUANTA-200, FEI Company, Hillsboro, OR, USA). Structural examination of synthesized materials was performed through a Shimadzu X-ray diffractometer. The diffractometer was set on the 2θ–θ scan setting with radiation of CuKα1 (λ = 1.5406 Å). Slits of 0.3 mm were applied for the source and detector sides. A voltage of 40 kV and a current of 30 mA were applied for X-ray generation. Then, diffraction patterns in the form of X-ray counts were collected utilizing a detector. The sample was rotated through 2θ = 8°–80° for this collection. Raman studies were carried out using an argon ion laser with a wavelength of 514.5 nm as the excitation source (Model Innova 70, Coherent, Santa Clara, CA, USA). TGA was performed using a TA instrument (TGA Q500, New Castle, DE, USA) with a ramp-rate of 10 °C/min in nitrogen atmosphere. A typical three-electrode cell system was utilized for performing electrochemical measurements. In the three-electrode cell system, a reference electrode (a saturated calomel electrode), a counter electrode (a platinum wire), and a working electrode (synthesized nanocomposites on nickel foam) were used. For the preparation of a working electrode, first, nickel foam was cleaned using 3 M HCl solution, followed by a cleaning using water and acetone. A paste consisting of the synthesized sample (80 wt.%), acetylene black (10 wt.%), and polyvinylidene difluoride (PVDF, 10 wt.%) was prepared using N-methyl pyrrolidinone (NMP) as a solvent. This paste was then applied to a pre-cleaned and weighted nickel foam. The paste was then dried under vacuum at 60 °C for 10 h. In the process of electrochemical testing, a 3 M KOH solution was utilized as an electrolyte. The electrochemical testing was performed using an electrochemical workstation (Versastat 4-500) from Princeton Applied Research, Oak Ridge, TN, USA. To examine the electrochemical attributes of these nanocomposites, cyclic voltammetry (CV) was performed.

3. Results and Discussion

The microstructures of MWCNTs, GONRs, polypyrrole, and nanocomposites of polypyrrole and GONRs were analyzed using scanning electron microscopy. The micrographs obtained are shown in Figures 1 and 2. The micrograph of pure MWCNTs showed tube-like structures (Figure 1a,b). The micrograph of pure GONRs (Figure 1c,d) revealed that the GONR layers were densely stacked as coralline-like flakes of irregular dimensions. On the other hand, the SEM image of PPy showed the segregation of PPy nanoparticles to form cauliflower-like structures (Figure 1e,f). A similar observation was found in previous studies as well [25]. The thermal degradation behavior of MWCNTs is given in Figure S1. As seen in the TGA curve, the MWCNTs showed a slow degradation residual weight of about 90% at 700 °C.

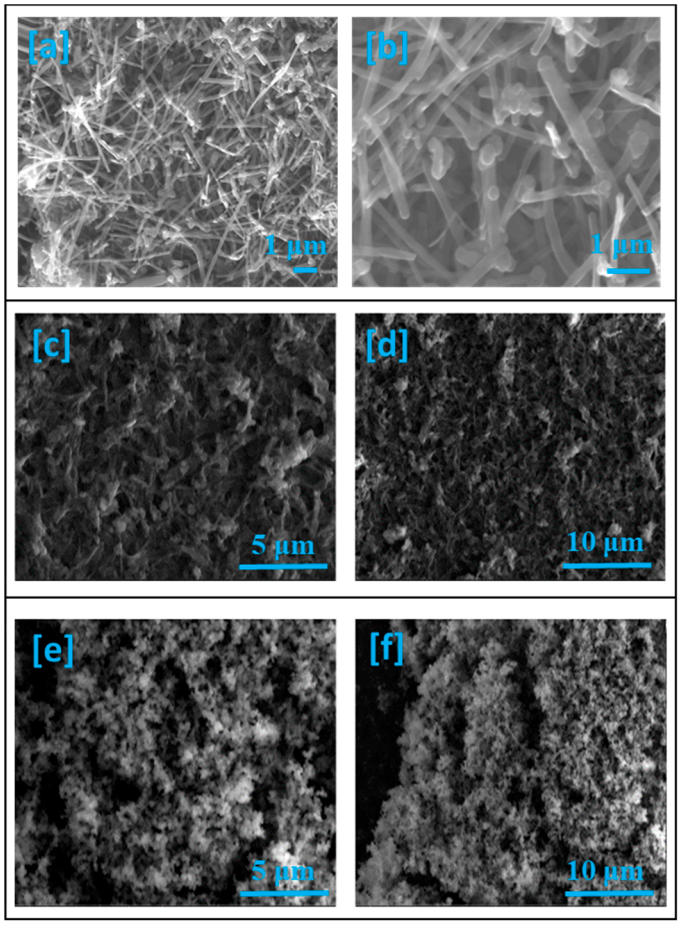

Figure 1. SEM images of (**a**,**b**) multiwall carbon nanotubes (MWCNTs); (**c**,**d**) graphene oxide nanoribbons (GONRs) and (**e**,**f**) polypyrrole (PPy) at various magnifications.

Figure 2a–c shows the microstructure of nanocomposites. It is evident from these images that the addition of GONRs led to the uniform growth of PPy nanoparticles on the GONRs. This could be a result of interactions (e.g., physical forces, hydrogen bonding, and pi-stacking) between GONRs and PPy [26]. Some aggregates of PPy nanoparticles could also be seen in the 3 PPyGONR composite. With a decreasing concentration of PPy, the roughness of stacked GONRs increased, and a large variety of pores were observed. Similar behavior was observed by Kovtyukhova et al. [27]. Such surface features can significantly improve the charge transfer characteristics and capacitance of the PPyGONR electrode [28].

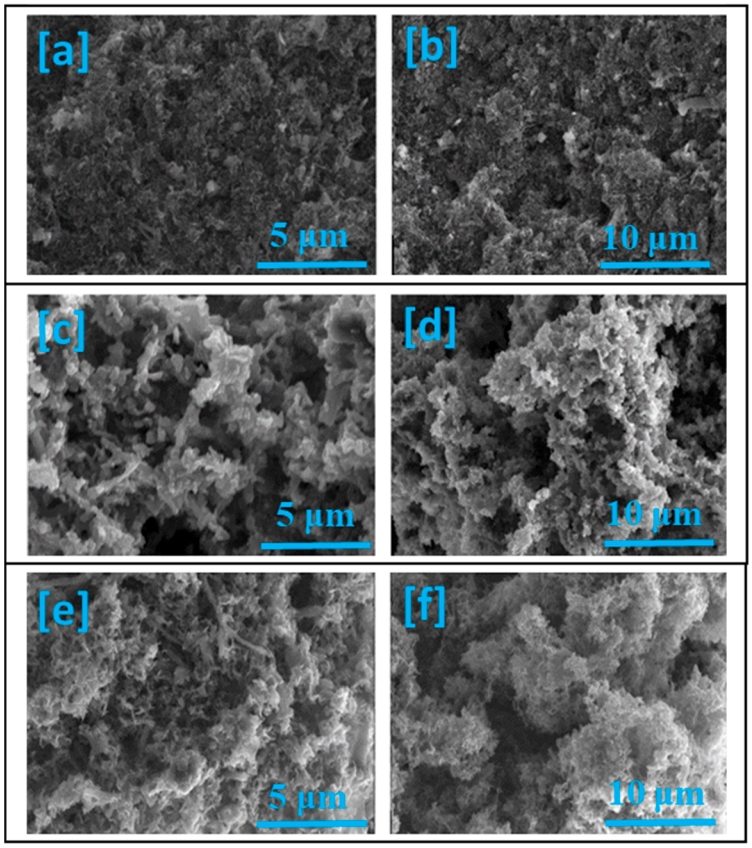

Figure 2. SEM images of PPy/GONR nanocomposites (PPyGONRs): (**a**,**b**) 0.5 PPyGONR, (**c**,**d**) 1.5 PPyGONR, and (**e**,**f**) 3 PPyGONR at various magnifications. Numerals indicate the weight ratio of GONRs in the nanocomposite, with the balance made up of PPy.

The unzipping and exfoliation of MWCNTs to form graphene oxide nanoribbons were investigated using XRD analysis. Figure 3 shows the XRD patterns of MWCNTs, GONRs, PPy, and their composites, respectively. In the case of MWCNTs (Figure 3a), the diffraction peaks in the vicinity of 25°, 45°, and 55° could be related to the (002), (100), and (004) planes of hexagonal graphite structure, respectively [29]. A strong reflection was obtained for GONRs around 2θ = 10°, corresponding to an interlayer spacing of 8.47, confirming the exfoliation of the sheets (Figure 3b). The shift of the (002) peak to low intensity was related to the attachment of residual functional groups having oxygen. These functional groups were bonded to the GONR sheets, and led to an increase in the interlayer spacing of the graphitic structure [26]. The diffraction patterns for pure PPy gave a broader peak in the region of 2θ = 20° to 28° and this indicated the formation of the amorphous phase of PPy (Figure 3c). The diffraction patterns for the PPy/GONR composites were very similar to that of PPy with no observation of diffraction peaks due to GONRs (Figure 3d–f). This could be due to the complete covering of GONRs by PPy and the low intensity of GONRs [26].

Raman spectroscopy was used to further characterize the samples. Figure 4 shows the Raman spectra of all the samples. Figure 4a,b shows the Raman spectra of MWCNTs and GONRs, respectively. GONRs showed two high-intensity bands around 1586 cm^{-1} and 1345 cm^{-1} which could be labeled as G and D bands of graphite or graphene, respectively. These bands were related to the in-plane optical vibration of graphite lattice and the first-order scattering of zone boundary phonons (E_{2g} mode) [25,30]. In the case of PPy, intense bands around 555 cm^{-1} and 1050 cm^{-1} were obtained (Figure 4b). These bands indicated the C–H out-of-plane and in-plane formation of PPy backbone [31]. The Raman spectra of the three composites are given in Figure 4c–e. The obtai0ned bands in the spectra of three composites had values of around 1560 cm^{-1} and 1340 cm^{-1} which corresponded to G and D bands of

the GONR. For all three samples, the broadness of bands was attributed to the interaction of PPy with graphene oxide (GO) sheets [31,32].

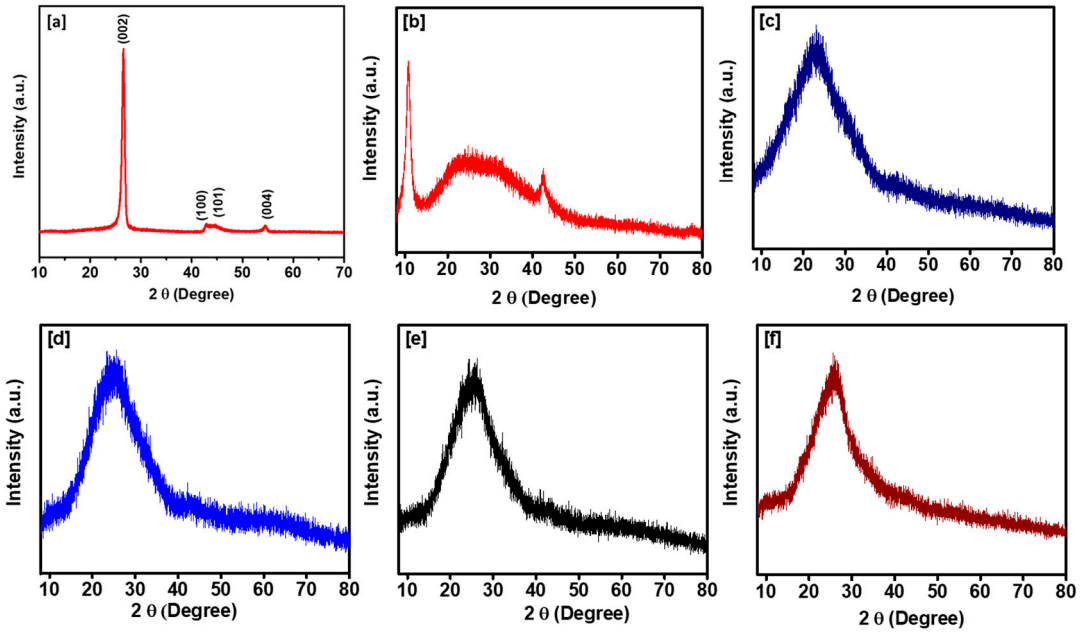

Figure 3. XRD patterns of (**a**) MWCNTs; (**b**) GONRs; (**c**) polypyrrole; (**d**) 0.5 PPyGONR; (**e**) 1.5 PPyGONR; and (**f**) 3 PPyGONR.

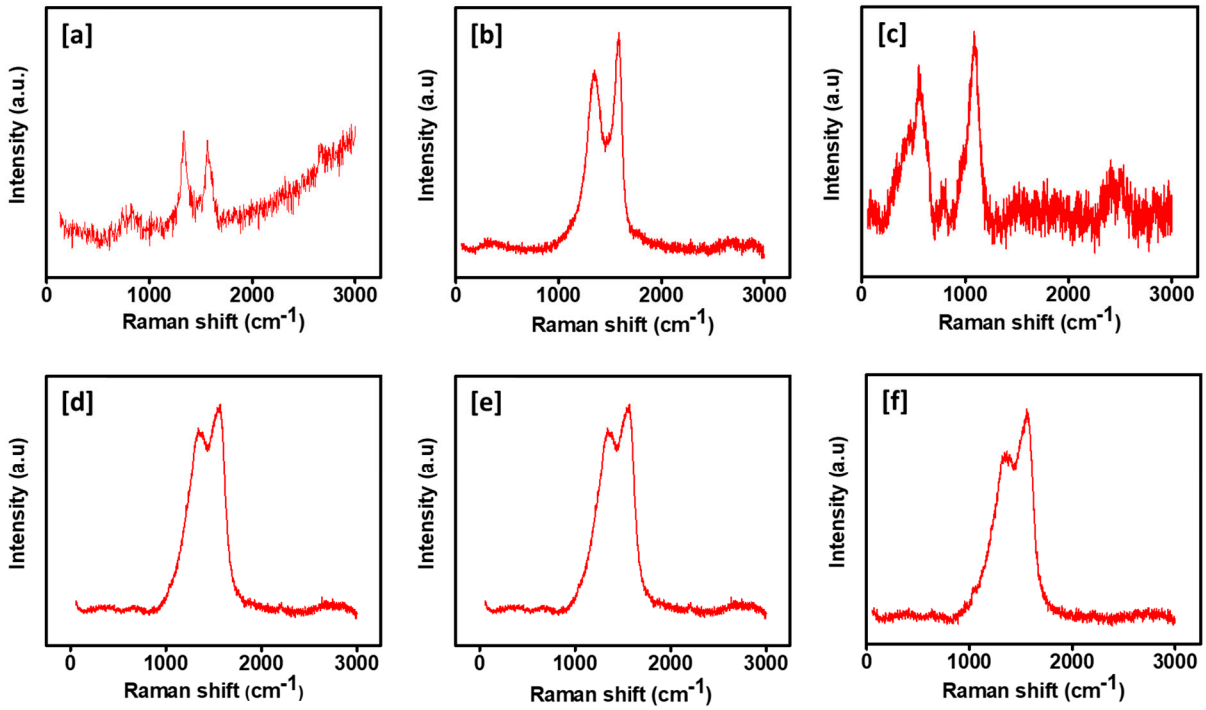

Figure 4. Raman spectra of (**a**) MWCNTs (**b**) GONRs, (**c**) PPy, (**d**) 0.5 PPyGONR, (**e**) 1.5 PPyGONR, and (**f**) 3 PPyGONR.

The purpose of this experiment was to study the electrochemical properties of synthesized GONRs, PPy, and their nanocomposites. Cyclic voltammetry measurements were performed in 3 M KOH electrolytes to investigate their electrochemical properties. Figure 5a–e shows the CV curves of GONRs, PPy, and their nanocomposites at various scan rates, respectively. The existence of redox peaks was

evident in the cyclic voltammograms of these samples, which indicated that the charge storage process in this system was dominated by the redox process. Specific capacitance of these electrodes was calculated using the measurements from the cyclic voltammetry data. The following is the expression used in the calculation of specific capacitance (C_{sp}) of the electrodes:

$$C_{sp} = \frac{Q}{\Delta V.\left(\frac{\partial \vartheta}{\partial t}\right).m}, \quad (1)$$

where $\partial\vartheta/\partial t$ is the scan rate, Q is the area under the CV curve, m is the mass of the sample and ΔV is the potential window of CV measurement. Figure 6a–e indicates the variation in specific capacitances as a function of scan rate for various samples. It was observed that specific capacitance decreased with an increase in scan rate, which could be due to insufficient time for redox reaction at higher scan rates. In this process, the electrochemical stability of the electrodes was evident, as the shapes of the CV curves were similar even at high scan rates. It was also observed that with the increase in scan rate, the peak position was shifted towards a higher potential. It can be inferred that the transfer of charge was the result of a diffusion-controlled process in these materials. GONRs and PPy showed specific capacitances of 415 and 522 F/g, respectively. The maximum value of specific capacitance was observed to be 2066 F/g for 3 PPyGONR. The specific capacitances of 0.5 PPyGONR and 1.5 PPyGONR were calculated to be 659 and 1368 F/g, respectively, which confirms that increasing the amount of GONR improved the electrochemical performance of the electrode. The high capacitance may be due to the highly porous structure of the composite and synergism between PPy and GONRs. Grover et al. synthesized graphene oxide nanoribbons (GONRs)- and reduced graphene oxide nanoribbons (RGONRs)-supported polyaniline (PANI) nanocomposites [33]. The highest specific capacitance found for GONR/PANI was 740 F/g and for RGONR/PANI it was 1180 F/g. Lacey reduced graphene oxide nanoribbons (LRGONRs) were chemically synthesized by Sahu et al. for supercapacitor applications. Using three-electrode cells, a high specific capacitance of 1042 F/g was reached at 1 mV/s [34]. A nanocomposite of polyaniline and graphene nanoribbons was studied by Li et al., who found a high specific capacitance of 340 F/g and a very stable performance [35]. As can be observed from other reported studies, our 3 PPyGONR is a promising material for supercapacitor applications.

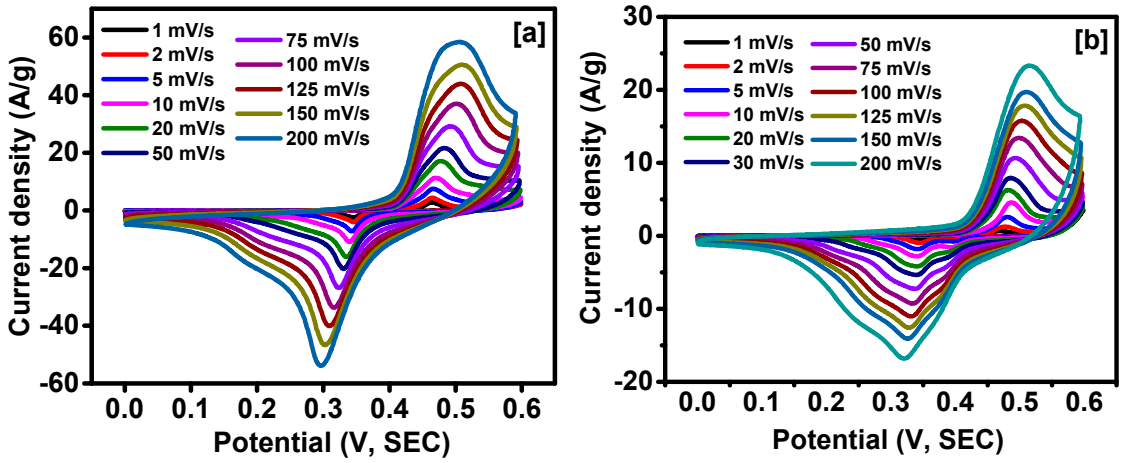

Figure 5. *Cont.*

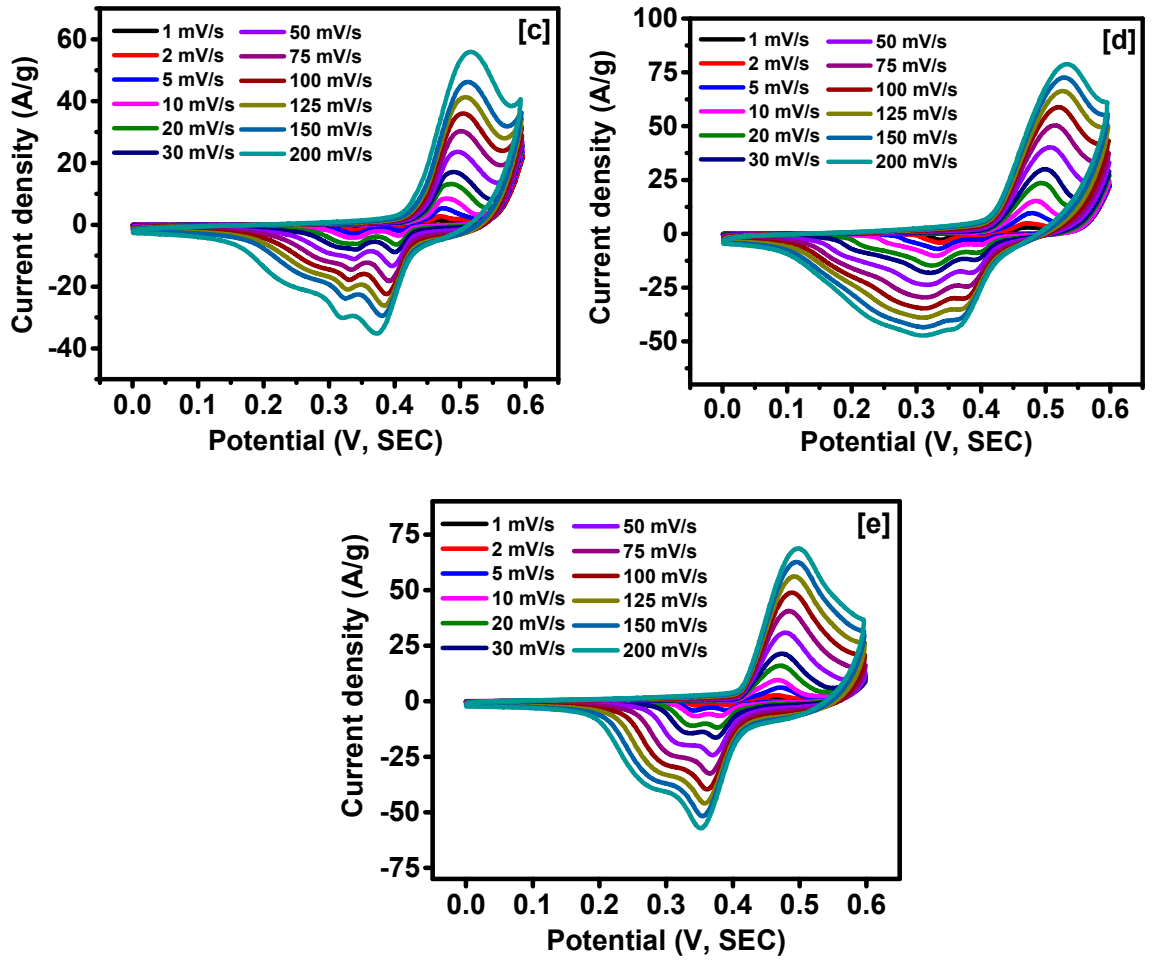

Figure 5. Cyclic voltammograms at various scan rates of (**a**) GONRs, (**b**) PPy, (**c**) 0.5 PPyGONR, (**d**) 1.5 PPyGONR, and (**e**) 3 PPyGONR.

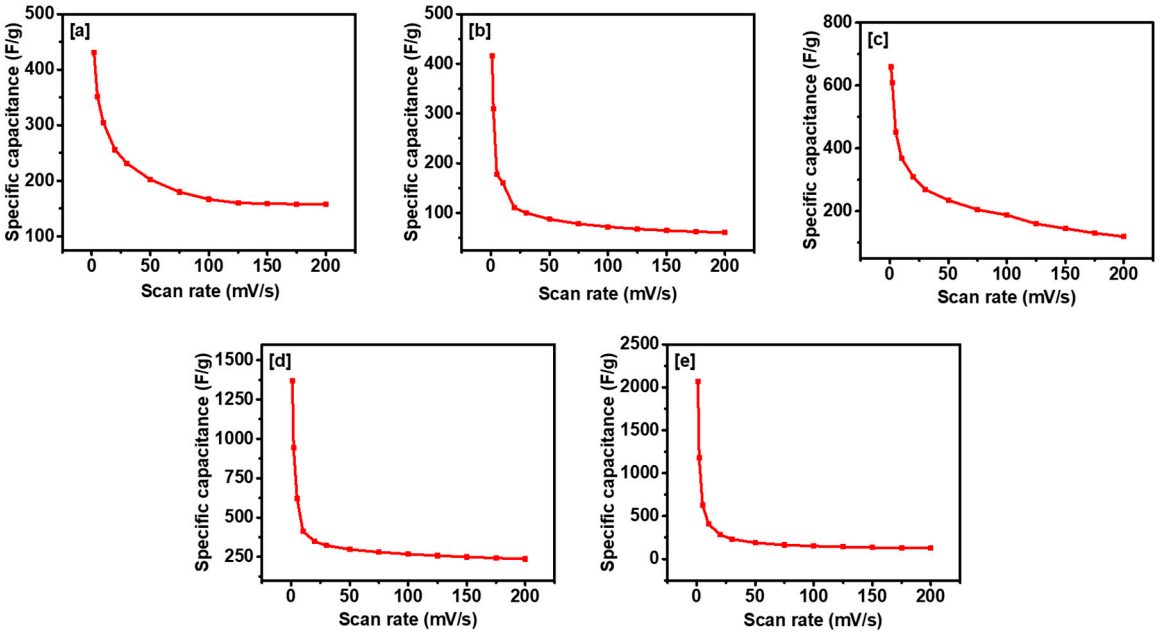

Figure 6. Variation of specific capacitance versus scan rate for (**a**) GONRs, (**b**) PPy, (**c**) 0.5 PPyGONR, (**d**) 1.5 PPyGONR, and (**e**) 3 PPyGONR.

4. Conclusions

Graphene nanoribbons were synthesized by unzipping MWCNTs. A facile chemical method was used to synthesize nanocomposites of PPy and GONRs. The synthesized materials were structurally characterized using SEM, XRD, and Raman spectroscopy. Using SEM, it was observed that the nanocomposites were made of polypyrrole nanoparticles. A large number of pores were observed in the composites. PPyGONR had a higher surface area than PPy, which improved the charge storage capacity of the nanocomposites. The electrochemical measurements showed the highest specific capacitance of 2066 F/g for 3 PPyGONR, which was observed to a decrease with increasing scan rates. The electrochemical results suggested that nanocomposites could be used as an electrode material for the fabrication of high-capacity supercapacitors. Finally, this study can be extended to the self-assembly of other conducting polymers and graphene nanoribbons through a simple route for various applications.

Supplementary Materials: The following are available online at http://www.mdpi.com/2311-5629/5/2/18/s1, Figure S1: TGA curve of MWCNTs.

Author Contributions: R.K.G. conceived of the project, designed the experiments, and finalized the manuscript. The first draft of the manuscript was written by J.A.D. and C.Z., S.R.M. provided SEM and Raman images/data. All authors reviewed and commented on the manuscript.

Funding: This research received no external funding.

Acknowledgments: Gupta expresses his sincere acknowledgment to the Polymer Chemistry Program and the Kansas Polymer Research Center, Pittsburg State University for providing financial and research support to complete this project. Mishra acknowledges the DRONE and Biologistic-FIT financial support by the University of Memphis.

Conflicts of Interest: The authors declare no conflict of interest.

References

1. Xu, X.; Liu, Y.; Dong, P.; Ajayan, P.M.; Shen, J.; Ye, M. Mesostructured $CuCo_2S_4$/$CuCo_2O_4$ nanoflowers as advanced electrodes for asymmetric supercapacitors. *J. Power Sources* **2018**, *400*, 96. [CrossRef]
2. Luo, Q.; Gu, Y.; Li, J.; Wang, N.; Lin, H. Efficient ternary cobalt spinel counter electrodes for quantum-dot sensitized solar cells. *J. Power Sources* **2016**, *312*, 93. [CrossRef]
3. Chen, H.; Hu, L.; Chen, M.; Yan, Y.; Wu, L. Nickel-Cobalt Layered Double Hydroxide Nanosheets for High-performance Supercapacitor Electrode Materials. *Adv. Funct. Mater.* **2014**, *24*, 934. [CrossRef]
4. Hsu, Y.-K.; Chen, Y.-C.; Lin, Y.-G. Synthesis of copper sulfide nanowire arrays for high-performance supercapacitors. *Electrochim. Acta* **2014**, *139*, 401. [CrossRef]
5. Yoo, J.J.; Balakrishnan, K.; Huang, J.; Meunier, V.; Sumpter, B.G.; Srivastava, A.; Conway, M.; Mohana Reddy, A.L.; Yu, J.; Vajtai, R.; et al. Ultrathin planar graphene supercapacitors. *Nano Lett.* **2011**, *11*, 1423. [CrossRef] [PubMed]
6. Chen, Z.; Yu, D.; Xiong, W.; Liu, P.; Liu, Y.; Dai, L. Graphene-based nanowire supercapacitors. *Langmuir* **2014**, *30*, 3567. [CrossRef]
7. Cruz-Silva, R.; Morelos-Gómez, A.; Vega-Díaz, S.; Tristán-López, F.; Elias, A.L.; Perea-López, N.; Muramatsu, H.; Hayashi, T.; Fujisawa, K.; Kim, Y.A.; et al. Formation of nitrogen-doped graphene nanoribbons via chemical unzipping. *ACS Nano* **2013**, *7*, 2192. [CrossRef] [PubMed]
8. Scuseria, G.E. Electromechanical properties of suspended graphene membranes. *Science* **2012**, *336*, 1557–1561.
9. Krepel, D.; Peralta, J.E.; Scuseria, G.E.; Hod, O. Graphene Nanoribbons-Based Ultrasensitive Chemical Detectors. *J. Phys. Chem. C* **2016**, *120*, 3791. [CrossRef]
10. Ahmed, S.; Ahmed, A.; Rafat, M. Nitrogen doped activated carbon from pea skin for high performance supercapacitor. *Mater. Res. Express* **2018**, *5*, 045508. [CrossRef]
11. Hu, J.; Qian, F.; Song, G.; Li, W.; Wang, L. Ultrafine MnO_2 Nanowire Arrays Grown on Carbon Fibers for High-Performance Supercapacitors. *Nanoscale Res. Lett.* **2016**, *11*, 469. [CrossRef]
12. Fan, L.Z.; Maier, J. High-performance polypyrrole electrode materials for redox supercapacitors. *Electrochem. Commun.* **2006**, *8*, 937. [CrossRef]
13. An, H.; Wang, Y.; Wang, X.; Zheng, L.; Wang, X.; Yi, L.; Bai, L.; Zhang, X. Polypyrrole/carbon aerogel composite materials for supercapacitor. *J. Power Sources* **2010**, *195*, 6964. [CrossRef]

14. Bibi, S.; Ullah, H.; Ahmad, S.M.; Ali Shah, A.U.; Bilal, S.; Tahir, A.A.; Ayub, K. Molecular and electronic structure elucidation of polypyrrole gas sensors. *J. Phys. Chem. C* **2015**, *119*, 15994. [CrossRef]
15. Lee, D.J.; Kim, E.; Kim, D.; Park, J.; Hong, S. Nano-storage wires. *ACS Nano* **2013**, *7*, 6906. [CrossRef]
16. Sultana, I.; Rahman, M.M.; Li, S.; Wang, J.; Wang, C.; Wallace, G.G.; Liu, H.K. Electrodeposited polypyrrole (PPy)/para (toluene sulfonic acid) (pTS) free-standing film for lithium secondary battery application. *Electrochim. Acta* **2012**, *60*, 201. [CrossRef]
17. Biswas, S.; Drzal, L.T. Multilayered nanoarchitecture of graphene nanosheets and polypyrrole nanowires for high performance supercapacitor electrodes. *Chem. Mater.* **2010**, *22*, 5667. [CrossRef]
18. Tran, V.C.; Sahoo, S.; Hwang, J.; Nguyen, V.Q.; Shim, J.-J. Poly(aniline-co-pyrrole)-spaced graphene aerogel for advanced supercapacitor electrodes. *J. Electroanal. Chem.* **2018**, *810*, 1541–1560. [CrossRef]
19. Sun, H.; She, P.; Xu, K.; Shang, Y.; Yin, S.; Liu, Z. A self-standing nanocomposite foam of polyaniline@reduced graphene oxide for flexible super-capacitors. *Synth. Met.* **2015**, *209*, 67–83. [CrossRef]
20. Bora, C.; Dolui, S.K. Fabrication of polypyrrole/graphene oxide nanocomposites by liquid/liquid interfacial polymerization and evaluation of their optical, electrical and electrochemical properties. *Polymer* **2012**, *53*, 923–932. [CrossRef]
21. Li, L.; Xia, K.; Li, L.; Shang, S.; Guo, Q.; Yan, G. Fabrication and characterization of free-standing polypyrrole/graphene oxide nanocomposite paper. *J. Nanopart. Res.* **2012**, *14*. [CrossRef]
22. Konwer, S.; Boruah, R.; Dolui, S.K. Studies on Conducting Polypyrrole/Graphene Oxide Composites as Supercapacitor Electrode. *J. Electron. Mater.* **2011**, *40*, 2248. [CrossRef]
23. Pham, H.D.; Pham, V.H.; Oh, E.-S.; Chung, J.S.; Kim, S. Synthesis of polypyrrole-reduced graphene oxide composites by in-situ photopolymerization and its application as a supercapacitor electrode. *Korean J. Chem. Eng.* **2012**, *29*, 125–129. [CrossRef]
24. Zhu, C.; Zhai, J.; Wen, D.; Dong, S. Graphene oxide/polypyrrole nanocomposites: One-step electrochemical doping, coating and synergistic effect for energy storage. *J. Mater. Chem.* **2012**, *22*, 63006. [CrossRef]
25. Wang, J.; Xu, Y.; Zhu, J.; Ren, P. Electrochemical in situ polymerization of reduced graphene oxide/polypyrrole composite with high power density. *J. Power Sources* **2012**, *208*, 138. [CrossRef]
26. Fan, L.Q.; Liu, G.J.; Wu, J.H.; Liu, L.; Lin, J.M.; Wei, Y.L. Asymmetric supercapacitor based on graphene oxide/polypyrrole composite and activated carbon electrodes. *Electrochim. Acta* **2014**, *137*, 26. [CrossRef]
27. Kovtyukhova, N.I. Layer-by-layer assembly of ultrathin composite films from micron-sized graphite oxide sheets and polycations. *Chem. Mater.* **1999**, *11*, 771. [CrossRef]
28. Jurewicz, K.; Delpeux, S.; Bertagna, V.; Béguin, F.; Frackowiak, E. Supercapacitors from nanotubes/polypyrrole composites. *Chem. Phys. Lett.* **2001**, *347*, 36. [CrossRef]
29. Schlange, A.; Dos Santos, A.R.; Kunz, U.; Turek, T. Continuous preparation of carbon-nanotubesupported platinum catalysts in a flow reactor directly heated by electric current. *Beilstein J. Org. Chem.* **2011**, *7*, 1412. [CrossRef]
30. Yang, Y.; Wang, C.; Yue, B.; Gambhir, S.; Too, C.O.; Wallace, G.G. Electrochemically synthesized polypyrrole/graphene composite film for lithium batteries. *Adv. Energy Mater.* **2012**, *2*, 266. [CrossRef]
31. Shannon, M.L.; Cole, D.I. Job satisfaction: RNs' status perceptions. *Nurs. Manag.* **1994**, *25*, 554. [CrossRef]
32. Scarlatescu, I.; Spunei, M.; Chis, A.; Negru, S.; Bunoiu, M.; Avram, N. Experimental dosimetric checkup under positioning errors according to gamma criterion. *UPB Sci. Bull. Ser. A Appl. Math. Phys.* **2018**, *80*, 271. [CrossRef]
33. Grover, S.; Goel, S.; Sahu, V.; Singh, G.; Sharma, R.K. Asymmetric Supercapacitive Characteristics of PANI Embedded Holey Graphene Nanoribbons. *ACS Sustain. Chem. Eng.* **2015**, *3*, 1460. [CrossRef]
34. Sahu, V.; Shekhar, S.; Sharma, R.K.; Singh, G. Ultrahigh performance supercapacitor from lacey reduced graphene oxide nanoribbons. *ACS Appl. Mater. Interfaces* **2015**, *7*, 3110. [CrossRef]
35. Li, L.; Raji, A.R.O.; Fei, H.; Yang, Y.; Samuel, E.L.G.; Tour, J.M. Nanocomposite of polyaniline nanorods grown on graphene nanoribbons for highly capacitive pseudocapacitors. *ACS Appl. Mater. Interfaces* **2013**, *5*, 6622. [CrossRef]